Calibration of TPM: Theory

From: Lin Han et al, to appear

1 Main Text

To gain more confidence in our understanding of the apparatus and analysis, we compared our experimental calibration curve to one we generated from a mathematical model of the system, following [1, 2]. The root-mean-square excursion of the projected bead location away from its tether point is controlled by various competing effects: (*i*) In the absence of any bead or wall, the chain's endpoint would execute 3D Brownian motion subject to a restoring force from the tether. (*ii*) But the bead's rotatory Brownian motion implies that its center, which is what we observe, lies a considerable distance away from the chain endpoint. (*iii*) The bead–wall exclusion pushes the bead upward, reducing its transverse excursions.

To account for all these effects, we modified the Gaussian sampling Monte Carlo technique previously used in [1, 2, 3] (see supplement). Our code generated many simulated DNA chains and bead orientations, applied the steric constraints [1], and reported the RMS deviation of the bead center from the attachment point. We applied a correction to this theoretical result, to account for the bead's motion during the rather long shutter time (about 31 msec, see supplement). Fig. 1 shows that an *a priori* calculation of the expected motion matches the data fairly well. The remaining discrepancy with our data may reflect unremoved instrumental drift, for example high-frequency motion that our Butterworth filter cannot distinguish from true Brownian motion. The variance of such noise would add in quadrature with the true Brownian motion.

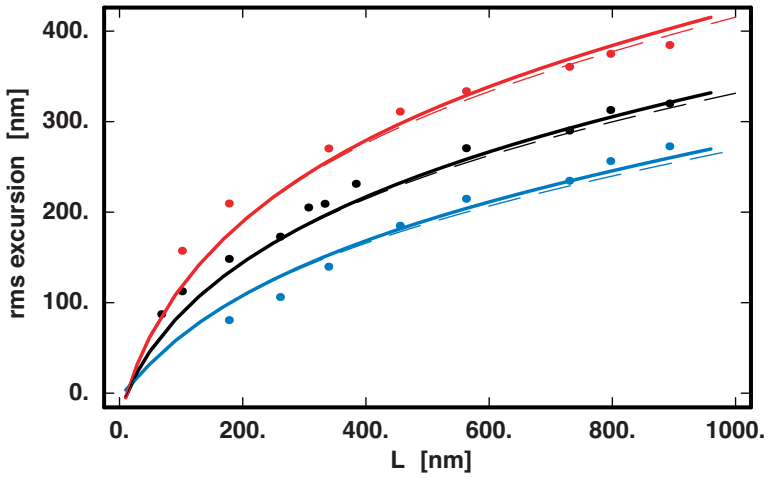

Figure 1: *Dots:* Experimental values for RMS motion of bead center for the three different bead sizes described in Table 1. Each dot represents the average of approximately 20–200 different observed beads with the given tether length. *Curves:* Theoretically predicted RMS motion, corrected for the blurring effect of our long shutter time. The solid curves assume $\xi = 50\,\mathrm{nm}$; the dashed curve assumes $\xi = 47\,\mathrm{nm}$. There are *no other fit parameters;* the theoretical model uses values for bead diameter given by the manufacturer's specification (Table 1).

2 Supplement

Here we describe the correction to the theoretical calibration curve in Fig. 1 to account for bead motion during a single frame exposure. The image of a static bead is a 2D distribution of intensity, $I_s(\mathbf{r} - \mathbf{r}_0)$, where $\mathbf{r}$ is the projected position in the focal plane. It reflects the "actual" bead image, the miscroscope pointspread function, uncertainties from finite pixel size, etc.

Finite shutter time blurs the image of a diffusing particle. As an extreme example, suppose the shutter were open for a time much longer than the bead's time to diffuse through its range of motion; then we would observe a blurred image centered on zero, and larger than the static image of the bead. In fact, some TPM implementations study this enlarged apparent bead image [4]. The bead-tracking method, which we use, discards the apparent image size and instead studies the apparent bead center position as a function of time. We now ask, how is this apparent bead center related to the true instantaneous bead position?

If we leave the shutter open only for a very short time, say 1 msec out of the total video frame time, then we may expect there would be very little blurring [2]. But in the present work, the shutter is open for almost the entire video frame; we need a correction to account for this fact. We first outline a simplified form of the correction, then a more accurate one.

Suppose we knew that at some time t the bead's true position is $\mathbf{r}_0$. This

is the quantity we want but can't observe directly. At a later time $t+\tau$, we only know the probability distribution function (pdf) of the bead's possible positions: It's centered on a new point $\mathbf{r}_\tau$. For tethered 2D Brownian motion, and infinitesimal τ, the new distribution $P(\mathbf{r};\tau)$ is a Gaussian of width $\sqrt{2D\tau}$ centered on $\mathbf{r}_\tau = \mathbf{r}_0 + (\mathbf{f}/\zeta)\tau$ where $\mathbf{f}$ is the restoring force of the tether, $\zeta = k_\mathrm{B}T/D = 6\pi\eta$ is the Stokes drag constant, and η is the viscosity of water. We can estimate the force by the Gaussian chain approximation, $\mathbf{f} = -k_\mathrm{B}T\mathbf{r}_0/(L\xi)$ where ξ is the persistence length. The average expected image at time $t+\tau$ is then the convolution of the static image I_s with P. This intensity distribution is centered at $\mathbf{r}_\tau$.

We can find the average blurred image by dividing the finite shutter time δt into small slices τ, finding the expected average image at each τ, and adding them all together. The average blurred image will be stretched relative to the static image, and its center will just be the average of the various $\mathbf{r}_\tau$. This center will be shifted radially inward relative to the initial $\mathbf{r}_0$, so call it $S(\rho_0)\mathbf{r}_0$, where $\rho_0 = |\mathbf{r}_0|$. $S(\rho_0) < 1$ is a scale factor function that we wish to find.

In the framework of the above approximations, the center ρ_τ obeys

$$\frac{d\rho}{d\tau} = v(\rho) = -\frac{1}{6\pi\eta R_b}\frac{k_\mathrm{B}T}{L\xi}\rho \tag{1}$$

Let $T = 6\pi\eta R_b L\xi/k_\mathrm{B}T$. So $\rho(\tau) = \rho_0 \mathrm{e}^{-\tau/T}$. The average of this center position over a finite shutter time δt is $S(\rho_0)\rho_0$ where

$$S(\rho_0) = \frac{T}{\delta t}[1 - \mathrm{e}^{-\delta t/T}] \tag{2}$$

Notice S is actually independent of ρ_0. For very small δt we get $S \to 1 - \frac{1}{2}(\delta t/T)$. For large δt, we have $S \to 0$.

We conclude that every report of $\mathbf{r}$ is systematically too small by a factor of S, which depends on the shutter time $\delta t = 31\,\mathrm{msec}$ and the tether length L (and other fixed quantities). If we want to predict the experimental data we should take the theoretical prediction, e.g. for $\sqrt{\langle\rho^2\rangle}$, and correct it, here by a factor of S. This correction is trivial to apply (comes out of the averaging sign), because S is independent of ρ_0.

The preceding discussion made some poor approximations. For example the drag constant is much bigger than the Stokes-law formula used above, due to wall effects. Nor is the tether end-end distance equal to ρ (there is also the distance from bead attachment to bead center, plus foreshortening due to projection to xy plane). Nor is the tether's entropic elasticity well represented by the Gaussian-chain formula. For all these reasons, we replaced Eqs. 1–2 by a phenomenological formula obtained from our data. We computed the average shift in the apparent position, from $\mathbf{r}$ on video frame N to $\mathbf{r}'$ on frame $N+2$, separated by $\Delta t = 65\,\mathrm{msec}$. We noted that $\mathbf{r}'$ was a radially symmetric function, that is, $\langle\mathbf{r}'\rangle$ points parallel to $\mathbf{r}$ with a reduced magnitude shown in Fig. 2 [5, 6]. To model this effect, we replaced Eq. 2 by the phenomenological form

$$\frac{d\rho}{d\tau} = -\frac{V_*}{L}\rho(1 - \alpha\rho) \tag{3}$$

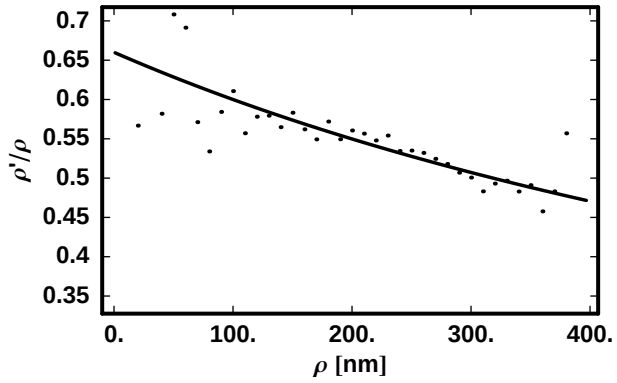

Figure 2: *Dots:* mean apparent radial bead displacement in a single time step, for DNA with $L = 901\,\mathrm{bp}$. The chosen time step is two video frames, or $\Delta t = 65.2\,\mathrm{msec}$. *Curve:* Phenomenological function for this displacement (see text).

As before, we then solved this equation to describe the migration of the centroid of positions that any given bead location will migrate to at a later time. If the true position at time 0 is ρ, then call the centroid of true positions later (at $t \neq 0$) $\hat{\rho}(\rho, t)$. The solution is determined by integrating Eq. 3, obtaining

$$\frac{\hat{\rho}}{\rho}\frac{1+\alpha\rho}{1+\alpha\hat{\rho}} = \mathrm{e}^{-V_* t/L}$$

which we then solve for $\hat{\rho}$.

To select appropriate values of V_* and α in Eq. 3, we examined the data in Fig. 2. During an exposure of duration δt, the apparent position is the average of $\hat{\rho}$ over the interval $(0, \delta t)$, which we call the corrected $\rho_{\mathrm{corr}}(\rho)$. The point-shift data of Fig. 2 give us $\rho_{\mathrm{corr}}(\rho_0)$ and $\rho_{\mathrm{corr}}(\rho')$ for various unobserved values of ρ_0, where $\rho' = \hat{\rho}(\rho_0, \Delta t)$. The curve in Fig. 2 is a scatterplot of such pairs, taking $V_* = 1.95\,\mathrm{nm/msec}$ and $\alpha = 0.0029/\mathrm{nm}$.

We applied the correction by modifying the Monte Carlo code to tabulate ρ_{corr}, not ρ. The RMS excursions of ρ_{corr} are shown in Fig. 1

References

[1] D. E. Segall, P. C. Nelson, and R. Phillips. Volume-exclusion effects in tethered-particle experiments: Bead size matters. *Physical Review Letters*, 96(8):088306–(1–4), 2006.

[2] P. C. Nelson, C. Zurla, D. Brogioli, J. F. Beausang, L. Finzi, and D. Dunlap. Tethered particle motion as a diagnostic of DNA tether length. *Journal of Physical Chemistry B*, 110(34):17260–17267, 2006.

[3] L. Czapla, D. Swigon, and W. K. Olson. Sequence-dependent effects in the cyclization of short DNA. *Journal of Chemical Theory and Computation*, 2(3):685–695, 2006.

[4] L. Finzi and J. Gelles. Measurement of lactose repressor-mediated loop formation and breakdown in single DNA-molecules. *Science*, 267(5196):378–380, 1995.

[5] J. F. Beausang, C. Zurla, C. Manzo, D. Dunlap, Laura Finzi, and P. C. Nelson. DNA looping kinetics analyzed using diffusive hidden Markov model. *Biophys. J.*, 92:L64–L66, 2007.

[6] J F Beausang and P C Nelson. Diffusive hidden markov model characterization of DNA looping dynamics in tethered particle experiments. Submitted; available on `arXiv.org`., 2007.